Available online at www.sciencedirect.com
ScienceDirect
Trans. Nonferrous Met. Soc. China 22(2012) s702−s706
Transactions of Nonferrous Metals Society of China
www.tnmsc.cn

Synthesis of Fe_3O_4-coated silica aerogel nanocomposites

Jun Sung LEE, Eun Jung LEE, Hae Jin HWANG

Devision of Materials Science and Engineering, Inha University, Incheon 402-751, Korea

Received 21 May 2012; accepted 5 November 2012

Abstract: Fe_3O_4:SiO_2 nanocomposite powders were synthesized by a two-step process, which included the precipitation of $FeCl_2$ and $FeCl_3$ and the gelation of silicic acid solution derived from water glass. At first, Fe_3O_4 nanoparticles having a crystallite size of 20 nm were obtained by controlling the ratio of Fe (II) and Fe (III) precursors. In the second step, Fe_3O_4 particles were embedded in SiO_2 matrix by the hydrolysis and subsequent condensation of the silicic acid solution containing Fe_3O_4 particles. It was found that the Fe_3O_4 nanoparticles homogenously disperse in the SiO_2 matrix. The Fe_3O_4:SiO_2 nanocomposite exhibited an enhanced thermal stability against oxidation compared with pure Fe_3O_4. FT-IR analysis indicates the presence of the Si—O—Fe bond in the Fe_3O_4:SiO_2 (1:10, mole fraction) nanocomposite.

Key words: nanocomposite; Fe_3O_4; SiO_2; sol−gel synthesis

1 Introduction

Magnetic nanoparticles have attracted much interest not only in the field of magnetic recording but also in the areas of medical field of magnetic sensing. Especially, nanoparticles of iron oxide are reported to be applicable as a material for use in drug delivery systems, magnetic resonance imaging, and cancer therapy [1−3].

On the other hand, most of the applications require magnetic particles to disperse in a non-magnetic matrix. The matrixes play an important role in determining physical properties of the composite nanoparticle in addition to providing a means of particle dispersion [1]. Another important characteristic of the matrix is to act as the protection of magnetic nanoparticles against corrosion or oxidation especially in the case of metallic nanoparticles [2]. Among carbon-based or oxide matrixes such as silica, alumina, titania or zeolite, silica can be a most suitable material for the matrix because of its non-toxicity, inertness to magnetic field and easiness to form cross-lined network structure [3,4].

Various techniques were proposed for synthesizing magnetic nanoparticles on which silica was coated. Stober process is the most well-known technique in which silica is produced via the hydrolysis of silicon-based alkoxide, for example, tetraethyl orthosilicate (TEOS) and subsequent condensation of silicic acid [5,6]. The other is based on the emulsion polymerization, in which aqueous droplets containing magnetic particles disperse in organic solvent with surfactant and then TEOS is added to the micro-emulsion to form silica particle on the magnetic particles. However, these methods are difficult to produce composite particles with sub-micron size.

In this work, magnetite (Fe_3O_4):silica (SiO_2) aerogel nanocomposite powders were synthesized using a novel synthesis route that consisted of coating magnetite particles with a silica aerogel through hydrolysis and condensation of water glass-derived silicic acid solution. Chemical compositions and morphologies of the prepared powder samples were measured by an X-ray diffractometer and a transmission electron microscope (TEM).

2 Experimental

Fe_3O_4 nanoparticles were prepared by co-precipitation of Fe_3O_4 from a mixture of $FeCl_2$ and $FeCl_3$ (1:2, molar ratio) upon addition of $NH_3{\cdot}H_2O$. In a typical reaction, 1.72 g $FeCl_2$ and 4.7 g $FeCl_3$ were mixed in 80 mL de-ionized water and heated to 80 °C in a three-necked flask. While vigorously stirring the reaction mixture, 10 mL of $NH_3{\cdot}H_2O$ was introduced by syringe,

Foundation item: Project (2011-0015512) supported by the National Research Foundation of Korea (NRF) Grant Funded by the Korea Government (MEST)
Corresponding author: Hae Jin HWANG; Tel: +82-32-860-7521; Fax: +82-32-862-4482; E-mail: hjhwang@inha.ac.kr
DOI: 10.1016/S1003-6326(12)61790-7

and the heating continued for 40 min. Black precipitate was produced immediately by adding $NH_3 \cdot H_2O$. The precipitation reaction is as follows:

$$Fe^{2+}+2Fe^{3+}+8OH^{-}=Fe_3O_4+4H_2O \quad (1)$$

The obtained Fe_3O_4 precipitate was washed repeatedly with de-ionized water until pH value decreased to 7 and then dried at 80 °C in an oven.

A sodium silicate solution (water glass) was used as a precursor to prepare the silicic acid. Water glass solution (Young Il Chemical, Korea) was diluted with distilled water to make an 8% (mass fraction) silicate solution. The solution was then passed through a column filled with an ion exchange resin (Amberite, IR-120H, H. Rohm & Hass Co., PA).

In this work, 3 samples with different molar ratios of Fe_3O_4 to SiO_2 (1:10, 1:20, 1:30) were prepared. An appropriate amount of Fe_3O_4 nanoparticles, which dispersed in de-ionized water, were added to the silicic acid solution. Then, $NH_3 \cdot H_2O$ was added to the silicic acid solution containing Fe_3O_4 particles until the pH value increased up to approximately 6. Gelation was carried out by heating the silicic acid solution up to 60 °C and the gelation process was finished within a few minutes. The obtained silica wet gel was dried at 80 °C for 3 d.

X-ray diffraction (XRD) patterns were taken using a diffractometer (DMAX−2500, Rigaku, Japan) with Ni-filtered Cu K_α radiation to confirm the crystallization of the sample. A Fourier transform infrared (FT−IR) spectroscope (FTS−165, Bio-Rad, USA) was used to confirm the surface chemical structure of the aerogels in the wave number range of 400−4000 cm^{-1}. The microstructures of Fe_3O_4 and Fe_3O_4:SiO_2 nanocomposite particles were examined by an electron microscope (JEM−4010, JEOL, Japan), operating at an accelerating voltage of 400 kV.

3 Results and discussion

Figure 1 shows typical XRD patterns of Fe_3O_4 and Fe_3O_4:SiO_2 composite powders. From Fig. 1(a), the obtained powder is found to be a pure Fe_3O_4. The peaks correspond to (220), (311), (222), (400), (422), (511), (440) and (533) of Fe_3O_4 crystalline structure. A broad diffraction peak near 2θ=23° is observed in the Fe_3O_4:SiO_2 composite powder (Fig. 1(b)). It may be attributed to the amorphous SiO_2. From Figs. 1(a) and (b), two powder samples show exactly the same XRD patterns except for the broad peak at 2θ=23°, which indicates that the crystallinity of the Fe_3O_4 particle embedded in SiO_2 is retained. The crystallite of the particle can be determined using classical Scherrer equation [7] from the X-ray wavelength and the width of the peak (full width at half maximum, FWHM). The crystallite sizes of Fe_3O_4 and Fe_3O_4:SiO_2 nanocomposite particle are estimated to be 17.6 and 18.0 nm, respectively.

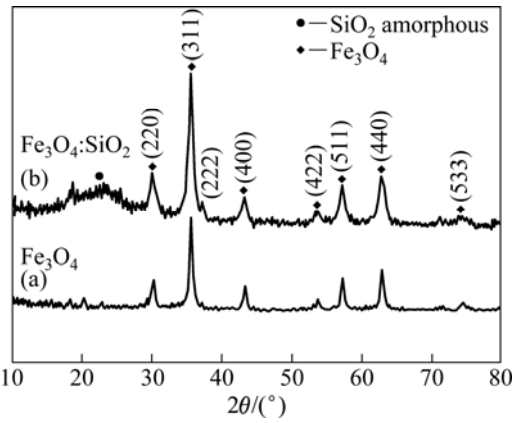

Fig. 1 XRD patterns of Fe_3O_4 (a) and Fe_3O_4:SiO_2 nanocomposite (b) powders

Fe_3O_4 and Fe_3O_4:SiO_2 composite powders with different amount of SiO_2 were prepared and the TEM images are shown in Fig. 2. The particle size of Fe_3O_4 is 10−20 nm in diameter and slightly agglomerated secondary particles form. In the case of the Fe_3O_4:SiO_2 composite powders, the agglomerated Fe_3O_4 particles are embedded in the SiO_2 aerogel matrix. In Figs. 2(b), (c) and (d), the dark particles are Fe_3O_4, while the grey ones are the SiO_2 aerogel matrix particles. The particle size of Fe_3O_4, which is embedded in the SiO_2 matrix, is estimated to be approximately 20 nm, suggesting that further agglomeration does not occur in the silicic acid solution containing Fe_3O_4 powders. The Fe_3O_4:SiO_2 nanocomposite particles retain the inherent characteristics of aerogels, including large surface area, through-connected porosity concentrated in the mesopore size range, and nanoscale particle sizes.

Figure 3 shows TEM images of Fe_3O_4:SiO_2 composite powders and the results of EDS analysis. The EDS analysis results confirm that black particles are Fe_3O_4 (Fig. 3(b), while the grey particles are SiO_2 (Fig. 3(c)). Figures 2 and 3 clearly exhibit that the Fe_3O_4 nanoparticles are embedded in the SiO_2 matrix, although they form agglomerated particles that range from a few tens nm to a few hundreds nm.

In order to investigate the oxidation behavior of the Fe_3O_4:SiO_2 nanocomposite powders, the as-synthesized powders were heat-treated at 400, 500, 600 and 700 °C in the air atmosphere. Figure 4 shows XRD patterns of the Fe_3O_4:SiO_2 nanocomposite powders heat-treated at different temperatures. For comparison, XRD patterns of the as-synthesized Fe_3O_4 and Fe_3O_4 heat-treated at 500 °C are also displayed. As is similar with Fig. 1, all the peaks of the composite powder samples heat-treated at

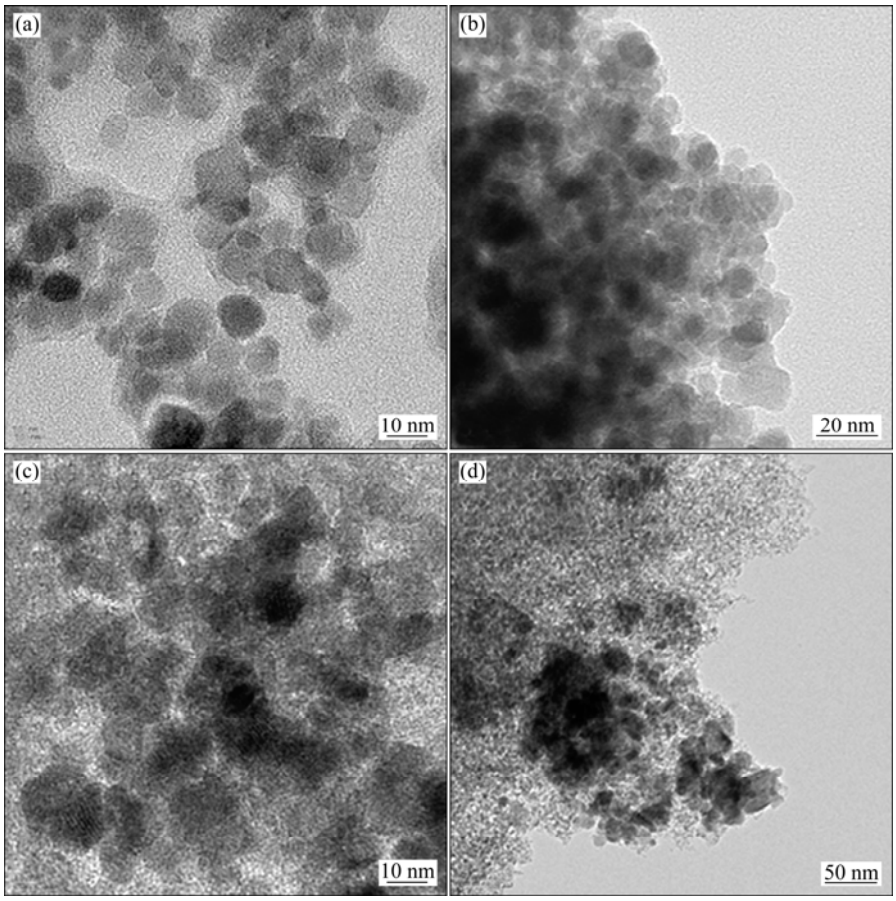

Fig. 2 TEM images of Fe_3O_4 and Fe_3O_4:SiO_2 nanocomposite powders: (a) Fe_3O_4; (b) $n(Fe_3O_4)$:$n(SiO_2)$=1:10; (c) $n(Fe_3O_4)$:$n(SiO_2)$=1:20; (d) $n(Fe_3O_4)$:$n(SiO_2)$=1:30

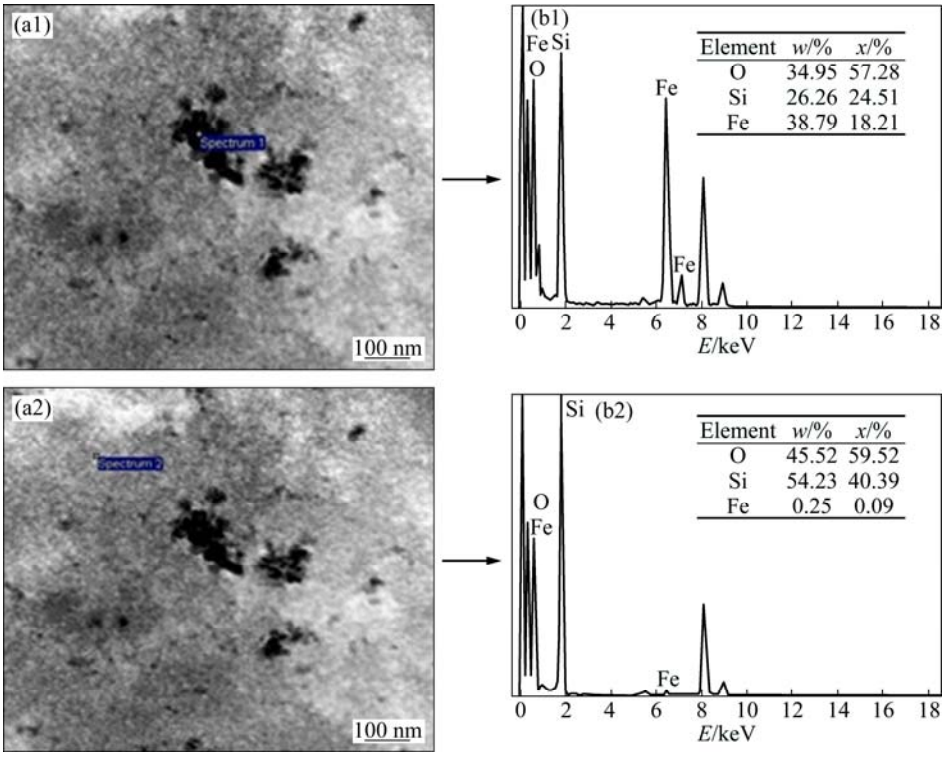

Fig. 3 TEM images of Fe_3O_4:SiO_2 nanocomposite powders (a1,a2), and EDS analysis results for black particle (b1) and grey particle (b2) in TEM images

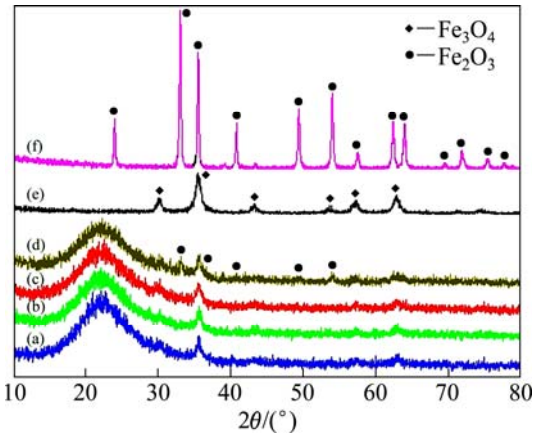

Fig. 4 XRD patterns of Fe_2O_3 and Fe_3O_4:SiO_2 nanocomposite powders heat-treated at various temperatures for 1 h in air atmosphere: (a) Fe_3O_4:SiO_2 heat-treated at 400 °C; (b) Fe_3O_4:SiO_2 heat-treated at 500 °C; (c) Fe_3O_4:SiO_2 heat-treated at 600 °C; (d) Fe_3O_4:SiO_2 heat-treated at 700 °C; (e) As-synthesized Fe_3O_4; (f) Fe_3O_4 heat-treated at 500 °C

400, 500 and 600 °C can be assigned to the crystalline Fe_3O_4 and amorphous SiO_2 phases. At 700 °C some peaks that are responsible for the Fe_2O_3 crystalline phase are observed, which indicates that the oxidation of Fe_3O_4 to Fe_2O_3 occurs between 600 and 700 °C. On the other hand, the Fe_3O_4 powder heat-treated at 500 °C is found to be pure Fe_2O_3, which means that pure Fe_3O_4 is oxidized to Fe_2O_3 at 500 °C. Thus, it can be inferred that the SiO_2 matrix can effectively suppress the oxidation of Fe_3O_4.

Figure 5 shows the FT-IR spectra of Fe_3O_4, SiO_2 and Fe_3O_4:SiO_2 nanocomposite powders. The broad band near 3400 cm^{-1} and small band at 1640 cm^{-1} that are confirmed in all the three samples can be assigned to the H—O—H stretching modes and bending vibration of the adsorbed water, respectively. The bands at 950 and 570 cm^{-1} may be associated with the Si—OH stretching [8,9]. These results suggest that the surfaces of the SiO_2 and Fe_3O_4:SiO_2 nanocomposite particles are hydrophilic. For the Fe_3O_4 particle, the bands near 1400, 600 and 300 cm^{-1} are characteristic of the Fe—O lattice vibrations [10,11].

On the other hand, the strong absorption bands near 1100 and 1220 cm^{-1} and the weak peak around 800 cm^{-1} are assigned to the asymmetry and symmetry bending modes of Si—O—Si, respectively. The strong band near 460 cm^{-1} is assigned to the Si—O—Si bending stretching mode. These peaks are characteristic peaks showing a typical silica aerogel network structure. GIRGINOVA et al [12] and DU et al [13] addressed that the bands at 574 and 943 cm^{-1} correspond to the stretching vibration of Si—O—Fe, respectively. For Fe_3O_4:SiO_2, the band at 950 cm^{-1} may be due to the Si—O—Fe bond in the nanocomposite particles. It appears that the Si—O—Fe characteristic band at 500 cm^{-1} is overlapped with the Si—O—Si and Si—OH bands.

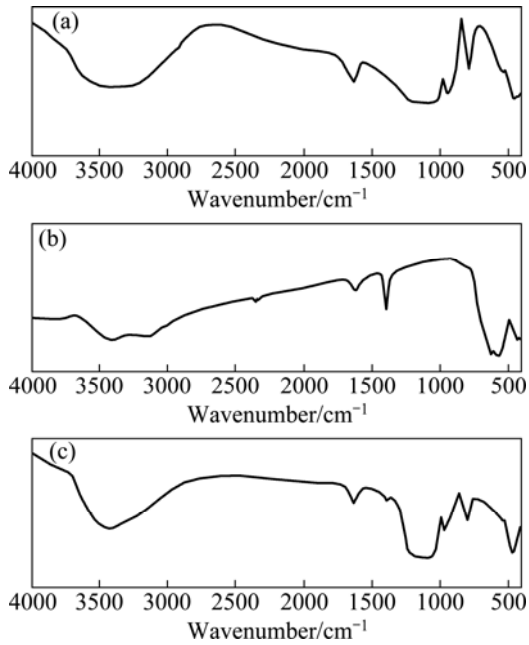

Fig. 5 FT-IR spectra of SiO_2 (a), Fe_3O_4 (b) and Fe_3O_4:SiO_2 (c) nanocomposite powders

4 Conclusions

Fe_3O_4:SiO_2 nanocomposite powders were synthesized by a two-step process, i.e., the precipitation and hydrolysis and condensation of a water glass-derived silicic acid solution with Fe_3O_4 nanoparticles. Fe_3O_4 nanoparticles are embedded in the SiO_2 matrix and FT-IR analysis suggests the chemical bond between Fe_3O_4 and SiO_2. The crystallite size of the Fe_3O_4:SiO_2 nanocomposites is about 20 nm. The oxidation resistance of the Fe_3O_4:SiO_2 nanocomposites was improved, which may be associated with the oxidation protective effect by the SiO_2 matrix.

References

[1] BERRY C C, CURTIS A S G. Functionalisation of magnetic nanoparticles for applications in biomedicine [J]. J Phys D: Appl Phys, 2003, 36: R198−R206.

[2] RUUGE E K, RUSETSKI A N. Magnetic fluids as drug carriers: Targeted transport of drugs by a magnetic field [J]. J Magn Magn Mater, 1993, 122: 335−339.

[3] POPE N M, ALSOP R C, CHANG Y A, SMITH A K. Evaluation of magnetic alginate beads as a solid support for positive selection of CD^{34+} cells [J]. J Biomed Mater Res, 1994, 2: 449−457.

[4] SOHN B H, COHEN R E, PAPAEFTHYMIOU G C. Magnetic properties of iron oxide nanoclusters within microdomains of block copolymers [J]. J Magn Magn Mater, 1998, 182: 216−224.

[5] KIM Y J, PEE J H, CHANG J H, CHOI K, KIM K J, JUNG D Y.

Silica effect on coloration of hematite nanoparticles for red pigments [J]. Chem Lett, 2009, 38: 842−843.

[6] HE Y P, WANG S Q, LI C R, MIAO Y M, WU Z Y, ZOU B S. Synthesis and characterization of functionalized silica-coated Fe_3O_4 superparamagnetic nanocrystals for biological applications [J]. J Phys D: Appl Phys, 2005, 38: 1342−1350.

[7] SHI Z L, DU C, YAO S H. Preparation and photocatalytic activity of cerium doped anatase titanium dioxide coated magnetite composite [J]. J Taiwan Inst Chem Eng, 2011, 42: 652−657.

[8] LU Y, YIN Y, MAYERS B, XIA Y. Modifying the surface properties of superparamagnetic iron oxide nanoparticles through a sol−gel approach [J]. Nano Lett, 2002, 2: 183−186.

[9] DENG Y, YANG W, WANG C, FU S. Dual-responsive polymer microspheres with well-defined core-shell structure [J]. Adv Mater, 2003, 15: 1729−1732.

[10] UVAROV V, POPOV I. Metrological characterization of X-ray diffraction methods for determination of crystallite size in nano-scale materials [J]. Mater Characterization, 2007, 58: 883−891.

[11] DARMAWAN A, SMART S, JULBE A, DINIZ DA COSTA J C. Iron oxide silica derived from sol-gel synthesis [J]. Materials, 2011, 4: 448−456.

[12] GIRGINOVA P I, DANIEL-DA-SILVA A L, LOPES C B, FIGUEIRA P, OTERO M, AMARAL V S, PEREIRA E, TRINDADE T. Silica coated magnetite particles for magnetic removal of Hg^{2+} from water [J]. J Colloid and Interface Sci, 2010, 345: 234−240.

[13] DU G H, LIU Z L, XIA X, CHU Q, ZHANG S M. Characterization and application of Fe_3O_4/SiO_2 nanocomposites [J]. J Sol-Gel Sci Techn, 2006, 39: 285−291.

(Edited by CHEN Wei-ping)